NASA Technical Memorandum 100915

Initial Condition Effect on Pressure Waves in an Axisymmetric Jet

Jeffrey H. Miles
NASA Lewis Research Center
Cleveland, Ohio

and

Ganesh Raman
Sverdrup Technology, Inc.
(Lewis Research Center Group)
NASA Lewis Research Center
Cleveland, Ohio

Prepared for the
First National Fluid Dynamics Congress
cosponsored by the AIAA, ASME, ASCE, SIAM, and APS
Cincinnati, Ohio, July 24–28, 1988

NASA

INITIAL CONDITIONAL EFFECT ON PRESSURE WAVES IN AN AXISYMMETRIC JET

Jeffrey H. Miles
NASA Lewis Research Center
Cleveland, Ohio 44135

and

Ganesh Raman
Sverdrup Technology, Inc.
(Lewis Research Center Group)
NASA Lewis Research Center
Cleveland, Ohio 44135

ABSTRACT

A pair of microphones (separated axially by 5.08 cm and laterally by 1.3 cm) are placed on either side of the jet centerline to investigate coherent pressure fluctuations in an axisymmetric jet at Strouhal numbers less than unity. Auto-spectra, transfer- function, and coherence measurements are made for a tripped and untripped boundary layer initial condition. It was found that coherent acoustic pressure waves originating in the upstream plenum chamber propagate a greater distance downstream for the tripped initial condition than for the untripped initial condition. In addition, for the tripped initial condition the development of the coherent hydrodynamic pressure waves shifts downstream.

INTRODUCTION

Jet excitation by low frequency acoustic waves (*i.e.* waves with Strouhal number based on the diameter, $St_d = fd/U$, in the range 0.2 to 0.6) can result in greater turbulent mixing, broadening of the mixing layer, shortening of the potential core, and modification of jet noise (Refs. 1–8). Research on the aeroacoustic excitation and control of shear flows has been reviewed in Refs. 9–11.

The effect of excitation on jet mixing was studied for cold jets in Refs. 1 and 8 and for hot jets in Ref. 7. These studies showed that excitation of a jet with a untripped initial condition has a much smaller effect on mixing than excitation of a jet with a tripped initial condition. In addition, these studies indicate that when using a constant level of excitation the most effective excitation frequency is at a St_d value near 0.5 which corresponds to the "preferred mode" or jet-column instability frequency introduced by Crow and Champagne (Ref. 2).

Many investigators studying the simple, average characteristic measures of the free shear layer, such as its width, momentum thickness, spread rate, similarity parameter, virtual origin location, and peak turbulence intensity have found large discrepancies in measurements which are now attributed to the effect of initial conditions for both two-dimensional free shear layers generated by splitter plates and free jet shear layers (Refs. 12 – 22). Based on these studies, trends in these measurements can be classified into cases where either the initial boundary layer is untripped or tripped.

It has frequently been suggested that the true explanation for the discrepancies between data obtained in different previous investigations of the characteristics of free shear layers has some connection with the large-scale coherent structures which might control the dynamics of the free jet (Refs. 15–21).

The axisymmetric shear flow in jets contains:

(1) large scale coherent structures that can be recognized visually;
(2) shear layer instability velocity and pressure waves;
(3) intense, connected, localized concentrations of vorticity (by definition the curl of the velocity).

The connections between these ways of looking at the jet is still a subject of research and debate (Refs. 23–25).

This paper discusses measurements of coherent pressure waves. Using the same jet that was used in the test program discussed in Ref. 8, two-point pressure measurements were made near the jet centerline to investigate large scale coherent structures, to obtain data which might be useful in validating computer codes, and to provide information on the unexcited jet which might be useful in improving the effect of excitation on jet mixing.

FACILITY AND PROCEDURE

FACILITY

The jet facility has a 8.89 cm inside diameter convergent nozzle at the end of a bellmouth which is attached to an excitation adaptor section. The excitation adaptor is attached to a 71 cm i.d. plenum chamber which is connected to a compressed-air supply.

For these tests a 0.95 cm felt flow filter and three screens are used in the plenum chamber to reduce turbulence. No other acoustic treatment was provided. The exit turbulence was about 0.15 percent.

The trip ring used to create a three-dimensional boundary layer has 82 saw-teeth which project about 4.76 mm into the flow and it is inserted where the diameter of the contracting section is 13.1 cm. The nozzle exit is 33 cm beyond the trip ring which should provide adequate length for the reattachment and development of the boundary layer. At the end of the convergent section of the nozzle is a constant area section which is 7.62 cm long. Since there is no axial area change, flow in this region should be free of pressure gradient effects.

The facility is the same as the one used in Ref. 8. The variation with Mach number of the exit boundary layer momentum thickness, θ^*, and shape factor are presented in Ref. 8 for the tripped and untripped case. The exit boundary layer shape factor is the ratio of displacement thickness, δ^*, to momentum thickness, $H^* = \delta^*/\theta^*$. For the tripped case, the shape factor is approximately 1.6 in the Mach number ranger $0.1 < M < 0.3$. For a flat-plate fully turbulent boundary layer using law-of-the wake relations yields a shape factor between 1.2 and 1.5. For the untripped case the shape factor varies from 2.2 at $M = 0.1$ to 1.8 at $M = 0.3$. For a flat-plate laminar boundary layer, the Blasius profile solution has a shape factor of 2.59. Thus, the untripped case is actually transitional rather than laminar and the tripped case should be considered as approaching a "fully turbulent" initial condition.

At $M = 0.3$ for the tripped case $(\theta^*/d) = 0.00657$ while for the untripped case $(\theta^*/d) = 0.0035$.

FACILITY OPERATION

The plenum temperature was 301K. The flow velocity was set to 104 m/s using a single hot wire to measure the nozzle exit velocity. All tests were made at the flow velocity corresponding to a Mach number of 0.30. The Reynolds number $(\rho V d/\mu)$ based on the nozzle diameter is 590,600.

The unsteady pressure measurements in the flow were made using conventional 0.635 cm microphones with pressure response cartridges and nose cones. The two microphones used were attached to a computer controlled traversing table. The microphone axial separation, Δx, was fixed at 5.08 cm. The lateral separation was 1.3 cm. The microphones were equidistant from the jet centerline and on opposite sides of the jet centerline. For these tests the midpoint of the two mikes is at $r/d = 0$. A side view is shown in Fig. 1. Data taken at four axial positions are presented herein. The data were obtained with the leading microphone sensing port at $x/d = 0.14, 0.86, 3$, and 9. The microphones were calibrated with a standard pistonphone at the start of the test.

Signals from the two microphones were simultaneously processed on-line by a 4 channel RAM- based disk driven digital signal processor to yield 400 point auto- and cross-spectra. This information was transferred to a mainframe computer for analysis. The cross-spectra and auto-spectra are used to calculate the transfer function magnitude and phase angle and the coherence between the two microphones in the flow. These results are then smoothed and enhanced to highlight data with a high coherence using the procedure described in Appendix A. The smoothed phase angle results are used to calculate the phase speed.

The number of averages used in these calculations was 50 and the frequency range used was 0 to 2000 Hz. Since data was available at 400 points the frequency spacing, Δf, was 5 Hz.

The conceptual basis for the data acquisition strategy is that the hydrodynamic pressure disturbances are a superposition of cylindrical harmonic travelling waves mixed in with flow and acoustic noise. The signals used in computing the cross-spectra must be phase coherent over the microphone separation distance since if the phases were random and independent the expected value of the cross-spectra would be zero.

In cylindrical coordinates the wave at x is assumed to be proportional to

$$e^{im\theta}$$

while the wave at $x + \Delta x$ is assumed to be proportional to

$$e^{im\theta + \Delta\theta}$$

For mode m the cross-spectrum at $x + \Delta x$ is related to the spectrum at x by the product of the signal at $x + \Delta x$ and the complex conjugate of the signal at x. Thus

$$G_m(x + \Delta x, x) = H_m G_m(x, x) e^{im\Delta\theta}$$

where H_m is the transfer function for mode m and $G_m(x, x)$ is the pressure spectrum at x. The instantaneous cross-spectrum is a weighted average of the modal cross-spectra. The measured cross- spectrum is the average of 50 instantaneous cross- spectra.

If the center of the propagating disturbance is on the jet centerline since the microphones are on opposite sides of the jet centerline it follows that

$$\Delta\theta = \pi$$

The sign of the even order cross-spectra is unchanged for even order modes since

$$e^{im(\theta+\pi)} = e^{im\theta}$$

if m is zero or even. However, for odd order cross-spectra

$$e^{im(\theta+\pi)} = -e^{im\theta}$$

if m is odd and the sign of the cross spectrum is changed. Consequently, near the nozzle the weighted average of the cross-spectra is not vary stationary and increasing the number of averages does not increase the smoothness of the cross-spectrum beyond a certain point. However, near the nozzle axisymmetric modes will be predominant and higher order modes will be more random since the nozzle is axisymmetric. Thus with this microphone geometry the axisymmetric modes will have a higher coherence near the nozzle. Consequently, the procedure described in Appendix A highlights the axisymmetric mode since it uses the coherence function as a weighting factor to smooth and enhance the data.

Far downstream, it is improbable that the center of a propagating hydrodynamic disturbance lies on the jet axis. It is much more likely that relative to the center of a propagating disturbance the two microphones are on the same side separated by a small angle. Consequently, the instantaneous cross-spectra will be a smoother average of all modes. Again, the procedure described in Appendix A highlights the dominant mode since it uses the coherence function as a weighting factor to smooth and enhance the data.

JET MOMENTUM THICKNESS

Results of measurements of the jet radial velocity profile made with hot wires at $x/d = 0.5, 1, 2, 4, 6, 8, 10,$ and 12 as part of the test program described in Ref. 8 were as expected. For example, the axial distribution of centerline velocity showed the velocity of the untripped jet decayed faster. This indicates the untripped jet mixed better than the tripped jet. The spectra results presented herein are scaled using a Strouhal number based on the jet diameter. However, for analytical calculations a Strouhal number based on jet momentum thickness, θ_j, is often of interest and the jet momentum thickness was calculated using the measured velocity profiles. At $x/d = 0.86, 3,$ and 9, the jet momentum thickness interpolated from the measured values is 0.345cm, 1.315cm, and 2.834cm for the untripped case and 0.448cm, 1.132cm and 2.687cm for the tripped case.

RESULTS

VALVE AND FLOW NOISE

The nozzle exit pressure auto-spectra for the untripped and tripped cases presented in Fig. 2 show acoustic tones from flow and valve noise. Frequencies of tones having significant amplitude are identified in Fig. 2. Also, Fig. 2 shows using the trip ring to change the boundary layer reduces the random flow noise and exposes the flow and valve noise tones.

MEASUREMENTS AT AXIAL STATIONS

For the tripped and untripped boundary layer inlet test conditions Figs. 3a–6a show pressure auto- spectra measured at $x/d = 0.14, 0.86, 3,$ and 9. Also shown for these two cases are the transfer function magnitudes (Figs. 3b–6b) (*i.e.* the ratio of the magnitude of the downstream phase correlated pressure to the upstream phase correlated pressure where the separation distance $\Delta x/d$ is 0.57) and coherence function (Figs. 3c–6c). In addition, the transfer function phase angle (Figs. 3d–6d) and the phase velocity (Figs. 3e–6e) calculated from the phase angle are shown. Only the curves shown in Figs. 3a–6a are unsmoothed and unenhanced. A continuous curve is used for the untripped boundary layer initial condition and a dashed curve is used for the tripped boundary layer initial condition.

PRESSURE AUTO-SPECTRA

The pressure auto-spectra is due to acoustic noise from the plenum, acoustic noise generated by the flow, and hydrodynamic pressure perturbations which are due to flow disturbance propagation. It includes both coherent and random disturbances.

Inspecting the pressure auto-spectra at different stations shows the tripped initial condition shifts the development of the coherent hydrodynamic waves downstream.

Figure 2 shows the pressure auto-spectrum is greater for the untripped case than for the tripped case in the range $0.0 < St_d < 0.9$. However, at $x/d = 0.14$ the pressure auto-spectrum is greater for the untripped case than for tripped case only in the range $0.4 < St_d < 0.8$ (Fig. 3a).

At $x/d = 0.86$, the increase of the pressure auto- spectrum of the untripped case is greater than that of the tripped case. Furthermore, it is greater than the tripped pressure auto-spectra in the range $0.0 < St_d < 1.0$ (Fig. 4a).

At $x/d = 3$, the untripped case pressure auto- spectrum has increased beyond its value at $x/d = 0.86$ and it remains greater than the tripped case pressure auto-spectrum in the range $0 < St_d < 0.4$. At higher Strouhal numbers the auto-spectra are similar (Fig. 5a).

At $x/d = 9$, the untripped and tripped case pressure auto-spectra are similar (Fig. 6 a).

For the tripped initial boundary layer initial condition the maturation of the pressure auto- spectrum lags behind the maturation of the pressure auto-spectrum for the untripped case. This indicates that for the untripped case not only are the random pressure disturbances greater at the nozzle exit but for this case the generation by the flow of acoustic and hydrodynamic noise is occurring nearer the nozzle.

COHERENCE FUNCTION MEASUREMENTS

In the following discussion the propagating waves are grouped into four Strouhal number bands based on the coherence function measurements (Figs. 3c–5c) and the tones observed in the nozzle exit auto-spectrum (Fig. 2). The bands will be discussed in increasing order of their Strouhal number range.

Acoustic waves dominate the pressure measurements in the first band which is in the Strouhal number range from 0 to 0.15. Thus, it is called the acoustic propagation band.

Another band of interest does not fall into a region of strong tones. It is in the Strouhal number range from 0.25 to 0.50. Disturbances in this band are associated with the "preferred mode" or the jet- column instability frequency introduced by Crow and Champagne (Ref. 2) and discussed in Refs. 25–28. Disturbances with frequencies in this band appear to be due to coupling of flow noise and instability waves and it will be called the flow noise band.

Near the nozzle ($x/d = 0.14, 0.86,$ and 3.0) the most significant band is in the Strouhal number range from 0.5 to 0.7. Disturbances with frequencies in this band appear to be due to coupling between the flow noise tones and instability waves and will be called the tonal band I.

A fourth band that appears in most cases is in the Strouhal number range from 0.75 to 1.0. Disturbances with frequencies in this band appear to be caused by direct excitation by tones in this region and it will called the tonal band II. However, these tones might also be harmonics of the tones in tonal band I.

One effect of the tripped boundary layer on wave propagation and the coherent structure of the jet can be determined by comparing the coherence of the tripped

case and untripped case. In tonal band I ($0.5 < St_d < 0.7$) and tonal band II ($0.75 < St_d < 1.0$) the tripped case coherence is larger than the untripped case coherence at $x/d = 0.14, 0.86,$ and 3 (Figs. 3c–5c) showing that phase related pressure waves excited by tones are propagating more coherently for the tripped initial condition. This may indicate that the valve and flow noise tones are having a greater effect on instability pressure wave propagation when the jet has a tripped initial condition.

Examining the coherence function at different stations again shows the tripped initial condition shifts the development of the coherent hydrodynamic waves downstream. In the flow noise band ($0.25 < St_d < 0.5$), the tripped and untripped case coherence are equal when the leading microphone is at $x/d = 0.14$ (Fig. 3c). When the leading microphone is at $x/d = 0.86$ the untripped case coherence is greater than the tripped case coherence (Fig. 4c). However, at $x/d = 3$ the tripped case coherence is greater than the untripped case coherence (Fig. 5c). When the leading microphone is at $x/d = 9$ the tripped and untripped case coherence are similar in this frequency band (Fig. 6c). This indicates the development of the tripped case coherence is delayed in the flow noise band relative to the development of the untripped case coherence.

TRANSFER FUNCTION

The transfer function magnitude is the ratio of the magnitude of the downstream phase correlated pressure to the magnitude of upstream phase correlated pressure where the separation distance $\Delta x/d$ is 0.57. It measures the amplification of the coherent pressure wave as it travels the separation distance.

While the values of the coherence are maximal in tonal band I, the values of the transfer function magnitude are maximal in the flow noise band.

Inspecting the pressure transfer function at different stations also shows the tripped initial condition shifts the development of the coherent hydrodynamic waves downstream. In the flow noise band and tonal band I the untripped case transfer function is larger when the leading microphone is at $x/d = 0.14$ (Fig. 3b). However, the tripped transfer function is larger in the flow noise band and tonal band I when the leading microphone is at $x/d = 0.86$ and 3 (Figs. 4b and 5b) and they are similar when the leading microphone is at $x/d = 9$. This indicates again that the tripped boundary layer initial condition delays development of the instability pressure waves.

PHASE ANGLE

From an acoustic/hydrodynamic wave propagation model, we have the following linear equations for the variation of the transfer function phase angle with Strouhal number for the axisymmetric mode acoustic wave leaving the nozzle, ψ_+, an axisymmetric mode acoustic wave travelling toward the nozzle, ψ_- , and an axisymmetric hydrodynamic wave, ψ, with constant phase velocity $c_{ph}/U = 0.64$:

$$\psi_+ = -360\frac{\Delta x}{c_o + U}\left(\frac{U}{d}\right)St_d = -47^o St_d \qquad (1)$$

$$\psi_- = 360\frac{\Delta x}{c_o - U}\left(\frac{U}{d}\right)St_d = 88^o St_d \qquad (2)$$

$$\psi = -360\frac{\Delta x}{c_{ph}}\left(\frac{U}{d}\right)St_d = -332^o St_d \qquad (3)$$

Consequently, for the axisymmetric mode acoustic waves leaving the nozzle the transfer function phase angle is less than -25^o at a Strouhal number of 0.5. For the axisymmetric mode hydrodynamic wave, the phase angle is -166^o.

The measured signal is composed of acoustic and shear layer instability pressure waves and the phase angle variation is governed by the dominant wave at each Strouhal number.

The phase angle measured with the leading microphone at $x/d = 0.14$ for the tripped and untripped case is shown in Fig. 3d. In the region $0.0 < St_d < 0.25$ the untripped phase angle is zero. For the tripped case, the phase angle fluctuates about -30 degrees in the region $0.0 < St_d < 0.25$. This indicates that the dominant wave propagating is an acoustic wave. Further evidence is found in the corresponding plot of the pressure transfer function magnitude and coherence (Figs. 3b and 3c) which indicates little coherent wave growth but high coherence.

In the range $0.25 < St_d < 0.4$, the untripped case phase angle gradually decreases. This indicates a decrease in the dominance of the acoustic waves.

The phase angle abruptly decreases between $0.46 < St_d < 0.6$. This is also a region where the transfer function peaks (Fig. 3b). This indicates that near the nozzle ($x/d = 0.14$) over the microphone separation distance ($\Delta x/d = 0.57$) a significant pressure instability wave is growing in this range of Strouhal numbers. Disturbances in this band are generally associated with the "preferred mode" or the jet-column instability frequency introduced by Crow and Champagne (Ref. 2) and discussed in Refs. 25–28. Disturbances with frequencies in this band are generally found only beyond $x/d = 4$. These results indicate that a significant coherent "preferred mode" pressure disturbance is present near the nozzle.

With the leading microphone at $x/d = 0.86, 3,$ and 9, the region where the phase angle is near zero is greatly reduced and the phase angle decreases with frequency almost linearly (Figs. 4d–6d). However, the true slope is not constant but corresponds to a frequency dependent phase velocity which will be discussed in the next section.

At low Strouhal numbers near the nozzle ($x/d = 0.14$) for the tripped and untripped case the acoustic wave dominates. However, only for the tripped case does the acoustic wave dominate in the Strouhal number range of 0.30 to 0.45. This indicates that for the untripped case the coherent acoustic wave acts at the nozzle exit and decays rapidly, while for the tripped case the coherent acoustic wave continues further downstream.

PHASE VELOCITY

Solving Eq. 3 for the ratio of the phase velocity to the jet exit velocity yields the formula used to calculate the normalized phase velocity from the smoothed pressure transfer function phase angle. When the relative phase velocity is less than unity the wave propagating at that frequency is assumed to be a mixture of waves dominated by the hydrodynamic wave. If the phase velocity is greater than or equal to unity the dominant wave is assumed to be acoustic. Calculated phase velocities are shown in Figs. 3e– 6e.

At $x/d = 3$ and 9, the ratio of the jet radius to jet momentum thickness, r/θ_j is less than 5. At these locations the phase velocity for both the untripped and tripped case increases in the Strouhal number range from 0.1 to 1 like the linear theory predicts for azimuthal hydrodynamic waves with r/θ_j less than 5 (Ref. 28). This suggests that the dominant hydrodynamic mode is azimuthal at these locations.

DISCUSSION

PREFERRED-FREQUENCY

The measured transfer functions show that an unusual degree of excitation near $St_d = 0.40$ at $x/d = 0.14, 0.86$ and 3 where the acoustic tones due to valve and flow noise are minimal. This dimensionless Strouhal number is the "preferred mode" for this jet and it has been suggested that it can be related by linear theory to a velocity profile and corresponding momentum boundary layer thickness which only occurs far from the nozzle at $x/d = 4$ to 5 (Ref. 25). If this is the case, then the following question remains: Why does one observe growth of waves near this frequency near the nozzle when near the nozzle the natural frequency of excitation based on the local velocity profile and momentum thickness is at a much higher frequency?. It has been suggested that this frequency is of importance near the nozzle due to acoustic feedback (Refs. 26 – 27) or inducement of velocity fluctuations at the nozzle by vortices in the jet shear layer (Ref. 28).

BOUNDARY LAYER INITIAL CONDITIONS

In tonal regions I and II $0.5 < St_d < 1.0$ the tripped case coherence is larger. Dziomba and Fiedler (Ref. 14) in a study of the effect of initial conditions on two-dimensional free shear layers also found the effect of resonance and blower noise was increased if the separating boundary layers were turbulent (tripped). They suggested that for a laminar boundary layer the periodic modulation forced on the shear layer at the trailing edge are randomized or damped by the strong stochastic processes of laminar turbulent transition and that this process does not occur at the edge if the boundary layer is already turbulent.

The same explanation might apply in the case of a nozzle. Note that the initial boundary layer longitudinal velocity fluctuation velocity intensity profiles peak away from the wall in a jet with a laminar boundary layer (Ref. 18, Fig. 1) and near the wall for a tripped boundary layer (Ref. 18, Fig. 9). In a free jet the longitudinal velocity fluctuation velocity intensity profiles peak at the inflection point of the mean velocity profile. Consequently, there is a smaller dislocation if the velocity profiles are tripped and the peak turbulent intensity is already at the nozzle wall. This smaller dislocation might reduce the randomization at the nozzle lip. This in turn might prevent the periodic modulations at the nozzle lip due to valve and flow noise tones from being damped by a large laminar turbulent transition process. The tripped boundary layer initial condition thus increases the sensitivity or receptivity of the flow to periodic perturbations. Thus the hydrodynamic pressure waves are more coherent for the tripped initial condition.

SELF-PRESERVATION

Hussain and Zedan show the self-preservation region of a jet with a laminar boundary layer inlet condition occurs at about $x/d = 1$ (Ref. 18, Figure 2) while for a turbulent boundary layer inlet condition it is delayed until $x/d = 2$ (Ref. 18, Figure 10). This is in good agreement with these dynamic pressure measurements which indicate that at $x/d = 0.86$ the coherent pressure wave propagation for the two cases is vastly different. For example, the turbulent case has a much larger pressure transfer function than the laminar case. At $x/d = 3$ the coherent pressure wave propagation for the two cases is similar and beyond $x/d = 3$ the self-preservation region for the turbulent case was found. These results indicate that the self-preservation region can not start until the pressure transfer function is less than unity.

CONCLUDING REMARKS

A pair of microphones (separated axially by 5.08 cm and laterally by 1.3 cm) are placed on either side of the jet centerline to investigate coherent pressure fluctuations in an axisymmetric jet at Strouhal numbers less than unity . Auto-spectra, transfer- function, and coherence measurements are made for a tripped and untripped boundary layer initial condition. The results show that coherent acoustic pressure waves originating in the plenum chamber propagate a greater distance downstream for the tripped initial condition than for the untripped initial condition.

In addition, the tripped boundary layer initial condition shifts development of the hydrodynamic wave measured with this microphone geometry downstream which results in a delay of:

(1) the decay of the coherence;
(2) the development of the pressure auto-spectra;
(3) the growth of the transfer function.

Also, these results indicate that a significant coherent "preferred mode" pressure disturbance is present near the nozzle.

As the measurement points move further from the nozzle exit , the tripped case and laminar case coherence, transfer function, and pressure auto- spectra become more similar and less dependent on the initial boundary condition. However, small differences exist even at $x/d = 9$.

Finally, it should be noted that the two microphone technique described here provides new insight into the propagation of the "preferred mode" and other coherent pressure waves in a jet as well as a diagnostic tool to look for naturally excited coherent pressure wave propagation which might interfere with externally applied excitation.

APPENDIX A

DATA SMOOTHING AND ENHANCEMENT

The coherence and transfer function data are smoothed using an 8 point weighted average. The coherence function is used to generate the weights.

The smoothed and enhanced transfer function phase angles ψ , transfer function magnitudes $\| H \|$, and coherence functions γ^2 are calculated as follows:

$$\psi_k = \begin{cases} (\psi_a)_k, & (\gamma_a^2)_k > 0.5 \\ (1-\eta)(\psi_a)_{k-1} + \eta S_1/S_4, & (\gamma_a^2)_k \leq 0.5 \text{ and } S_4 > 0.0 \\ (\psi_a)_{k-1}, & (\gamma_a^2)_k \leq 0.5 \text{ and } S_4 = 0.0 \end{cases} \quad \text{(A 1)}$$

$$\| H_k \| = \begin{cases} (\| H_a \|)_k, & (\gamma_a^2)_k > 0.5 \\ (1-\eta)(\| H_a \|)_{k-1} + \eta S_2/S_4, & (\gamma_a^2)_k \leq 0.5 \text{ and } S_4 > 0.0 \\ (\| H_a \|)_{k-1}, & (\gamma_a^2)_k \leq 0.5 \text{ and } S_4 = 0.0 \end{cases} \quad \text{(A 2)}$$

$$\gamma_k^2 = \begin{cases} (\gamma_a^2)_k, & (\gamma_a^2)_k > 0.5 \\ (1-\eta)(\gamma_a^2)_{k-1} + \eta S_3/S_4, & (\gamma_a^2)_k \leq 0.5 \text{ and } S_4 > 0.0 \\ (\gamma^2)_{k-1}, & (\gamma_a^2)_k \leq 0.5 \text{ and } S_4 = 0.0 \end{cases} \quad \text{(A 3)}$$

where a value of 0.1 was used for η.

For $l = k$ to $k-7$ if $(\psi_a)_{k-1} - (\psi_a)_l > 180$ then

$$S_1 = S_2 = S_3 = S_4 = 0. \quad \text{(A 4)}$$

For $(\psi_a)_{k-1} - (\psi_a)_l \leq 180$ then

$$S_1 = \sum_{j=k}^{j=k-7} wt_j (\psi_a)_j \quad \text{(A 5)}$$

$$S_2 = \sum_{j=k}^{j=k-7} wt_j (\| H_a \|)_j \quad \text{(A 6)}$$

$$S_3 = \sum_{j=k}^{j=k-7} wt_j (\gamma_a^2)_j \quad \text{(A 7)}$$

$$S_4 = \sum_{j=k}^{j=k-7} wt_j \quad \text{(A 8)}$$

where

$$wt_j = \begin{cases} 1, & \gamma_a^2 \geq 0.5 \\ \gamma_a^2, & 0.01 < \gamma_a^2 < 0.5 \\ 0.01, & \gamma_a^2 < 0.01 \ . \end{cases} \quad \text{(A 9)}$$

REFERENCES

1. Vlasov, E.V. and Ginevskii, A.S., "Acoustic Modification of the Aerodynamic Characteristics of a Turbulent Jet," Fluid Dynamics, Vol. 2., No. 4, July-Aug. 1967, pp. 93-96.
2. Crow, S.C. and Chamapagne, F.H., "Orderly Structure in Jet Turbulence," Journal of Fluid Mechanics, Vol. 48, Pt. 3, Aug. 16, 1971, pp. 547-591.
3. Vlasov, E.V. and Ginevskii, A.S., "Generation and Suppression of Turbulence in an Axisymmetric Turbulent Jet Under an Acoustic Effect," Fluid Dynamics, Vol. 8, No. 6, Nov.-Dec. 1973, pp. 881-885.
4. Moore, C.J., "The Role of Shear-Layer Instability Waves in Jet Exhaust Noise," Journal of Fluid Mechanics, Vol. 80, Pt. 2, Apr. 25, 1977, pp. 321-367.
5. Schmidt, C., "Aerodynamic Characterization of Excited Jets," Journal of Sound and Vibration, Vol. 61, No. 1, Nov. 8, 1978, pp. 148-152.
6. Jubelin, B., "New Experimental Studies on Jet Noise Amplification," AIAA Paper 80-0961, June 1980.
7. Lepicovsky, J. and Brown, W.H., "Effects of Nozzle-Exit Boundary-Layer Conditions on Excitability of Heated Free Jets," AIAA Paper 87-2723, Oct. 1987.
8. Raman, G., Zaman, K.B.M.Q., and Rice, E.J., "Initial Turbulence Effect on Jet Evolution With and Without Tonal Excitation," AIAA Paper 87-2725, Oct. 1987. (NASA TM-100178).
9. Vlasov, E.V. and Ginevskii, A.S., "The Aeroacoustic Interaction Problem (Review)," Soviet Physics Acoustics, Vol. 26, No. 1, Jan.-Feb. 1980, pp. 1-7.
10. Stone, J.R. and McKinzie, D.J. Jr., "Acoustic Excitation—A Promising New Means of Controlling Shear Layers," NASA TM-83772, 1984.
11. Rice, E.J. and Zaman, K.B.M.Q., "Control of Shear Flows by Artificial Excitation," AIAA Paper 87-2722, Oct. 1987. (NASA TM-100201).
12. Batt, R.G., "Some Measurements on the Effect of Tripping the Two-Dimensional Shear Layer," AIAA Journal, Vol. 13, No. 2, Feb. 1975, pp. 245-247.
13. Browand, F.K. and Latigo, B.O., "Growth of the Two-Dimensional Mixing Layer from a Turbulent and Nonturbulent Boundary Layer," Physics of Fluids, Vol. 22, No. 6, June 1979, pp. 1011-1019.
14. Dziomba, B. and Fiedler, H.E., "Effect of Initial Condition on Two-Dimensional Free Shear Layers," Journal of Fluid Mechanics, Vol. 152, Mar. 1985, pp. 419-442.
15. Bradshaw, P., "The Effect of Initial Conditions on the Development of a Free Shear Layer," Journal of Fluid Mechanics, Vol. 26, Pt. 2, Oct. 1966., pp. 225-236.
16. Hussain, A.K.M.F. and Clark, A.R., "Upstream Influence on the Near Field of a Plane Turbulent Jet," Physics of Fluids, Vol. 20, No. 9, Sept. 1977, pp. 1416-1426.
17. Hussain, A.K.M.F., "Initial Condition Effect on Free Turbulent Shear Flows," Structure and Mechanisms of Turbulence I, H. Fiedler, ed., Springer, New York, 1978, pp. 103-107.

18. Hussain, A.K.M.F. and Zedan, M.F., "Effects of the Initial Condition on the Axisymmetric Free Shear Layer: Effects of the Initial Momentum Thickness," Physics of Fluids, Vol. 21, No. 7, July 1978, pp. 1100-1112.
19. Hussain, A.K.M.F. and Zedan, M.F., "Effects of the Initial Condition on the Axisymmetric Free Shear Layer: Effect of the Initial Fluctuation Level," Physics of Fluids, Vol. 21, No. 9, Sept. 1978, pp. 1475-1481.
20. Husain, Z.D. and Hussain, A.K.M.F., "Axisymmetric Mixing Layer: Influence of the Initial and Boundary Conditions," AIAA Journal, Vol. 17, No. 1, Jan. 1979, pp. 48-55.
21. Hussain, A.K.M.F. and Husain, Z.D., "Turbulence Structure in the Axisymmetric Free Mixing Layer," AIAA Journal, Vol. 18, No. 12, Dec. 1980, pp. 1462-1469.
22. Hill, W.G. Jr., Jenkins, R.C., and Gilbert, B.L., "Effects on the Initial Boundary-Layer State on Turbulent Jet Mixing," AIAA Journal, Vol. 14, No. 11, Nov. 1976, pp. 1513-1514.
23. Hussain, A.K.M.F., "Coherent Structures-Reality and Myth," Physics of Fluids, Vol. 26, No. 10, Oct. 1983, pp. 2816-2850.
24. Hussain, A.K.M.F., "Coherent Structures and Turbulence," Journal of Fluid Mechanics, Vol. 173, Dec. 1986, pp. 303-356.
25. Wygnanski, I.J. and Petersen, R.A., "Coherent Motion in Excited Free Shear Flows," AIAA Journal, Vol. 25, No. 2, Feb. 1987, pp. 201-213.
26. Kibens, V., "Discrete Noise Spectrum Generated by an Acoustically Excited Jet," AIAA Journal, Vol. 18, No. 4, Apr. 1980, pp. 434-441.
27. Gutmark, E. and Ho, C.M., "Preferred Modes and the Spreading Rates of Jets," Physics of Fluids, Vol. 26, No. 10, Oct. 1983, pp. 2932-2938.
28. Michalke, A., "Survey on Jet Instability Theory," Progress in Aerospace Sciences, Vol. 21, No. 3, 1984, pp. 159-199.

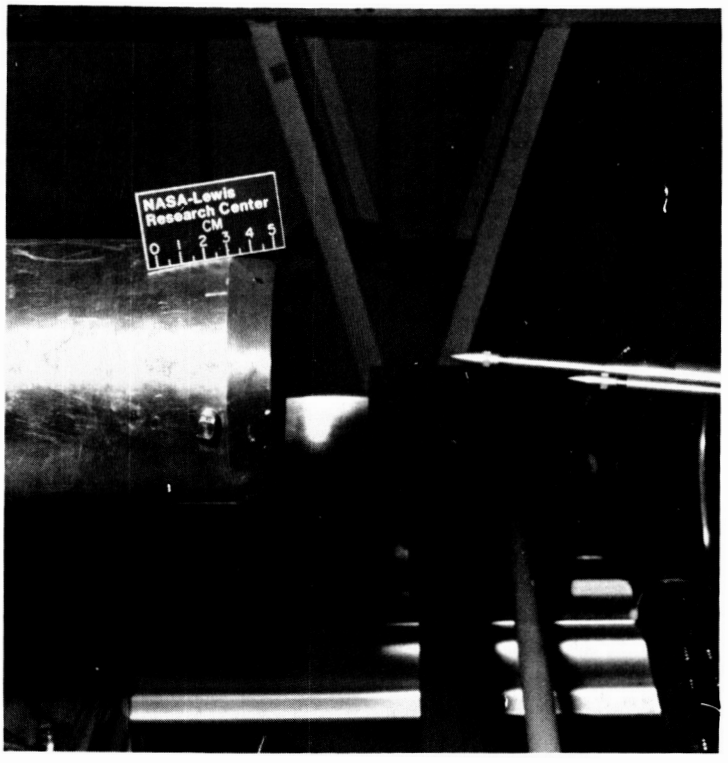

FIGURE 1. - SIDE VIEW OF MICROPHONES.

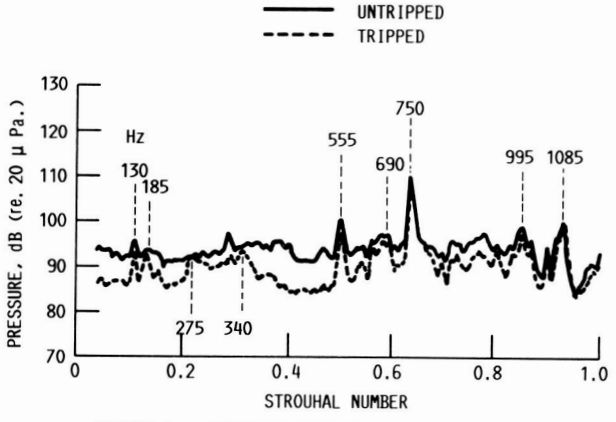

FIGURE 2. - PRESSURE AUTO-SPECTRUM AT NOZZLE EXIT.
(x/d = 0, r/d = 0, M = 0.3.)

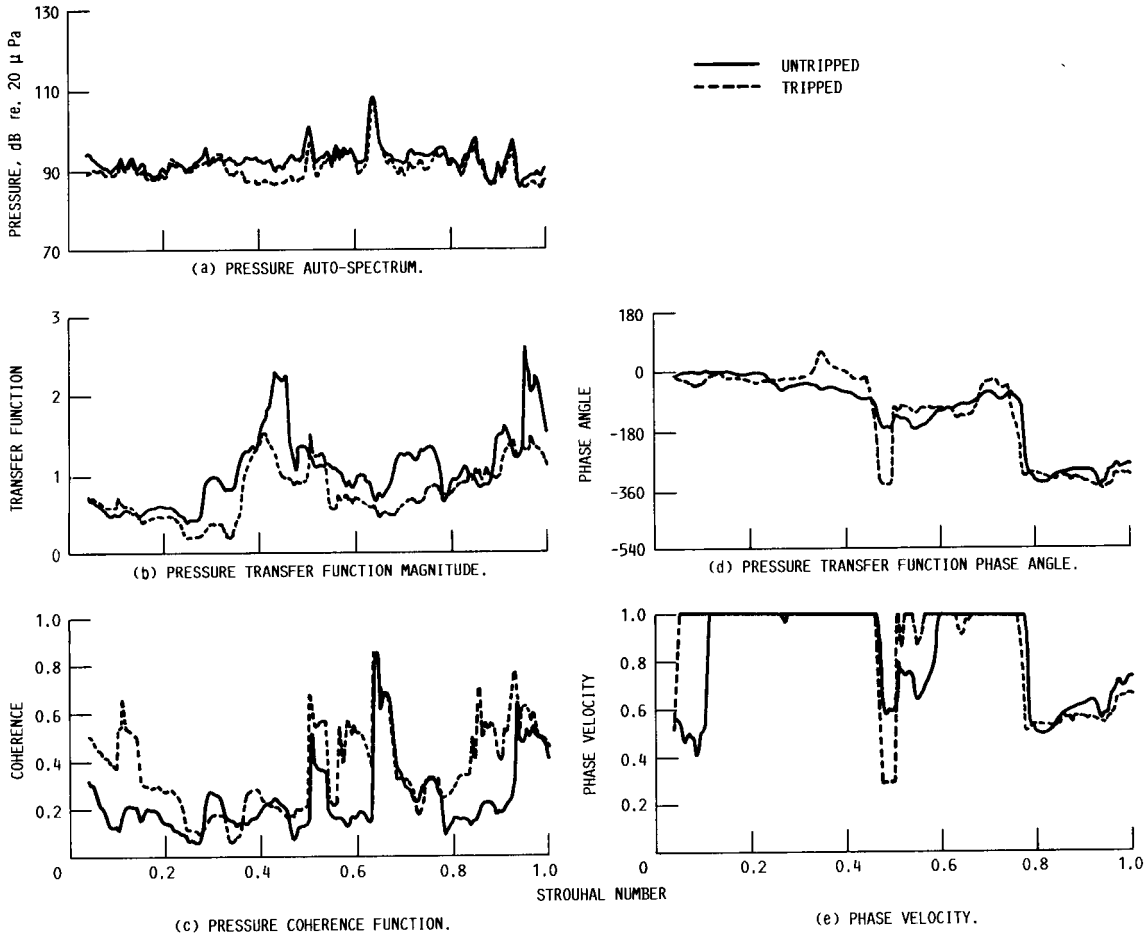

FIGURE 3. - MEASUREMENTS AT x/d = 0.14. (r/d = 0, M = 0.3.)

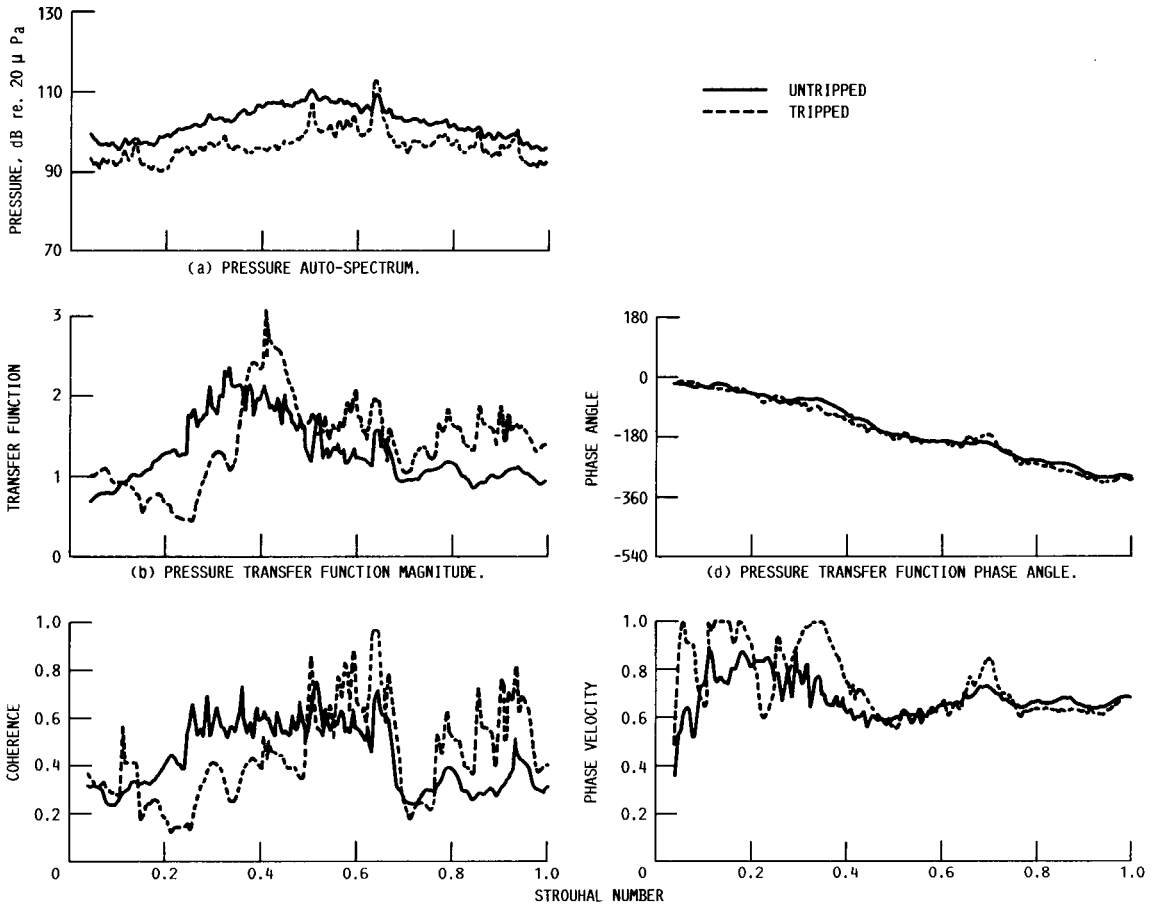

(a) PRESSURE AUTO-SPECTRUM.

(b) PRESSURE TRANSFER FUNCTION MAGNITUDE.

(d) PRESSURE TRANSFER FUNCTION PHASE ANGLE.

(c) PRESSURE COHERENCE FUNCTION.

(e) PHASE VELOCITY.

FIGURE 4. - MEASUREMENTS AT x/d = 0.86. (r/d = 0, M = 0.3.)

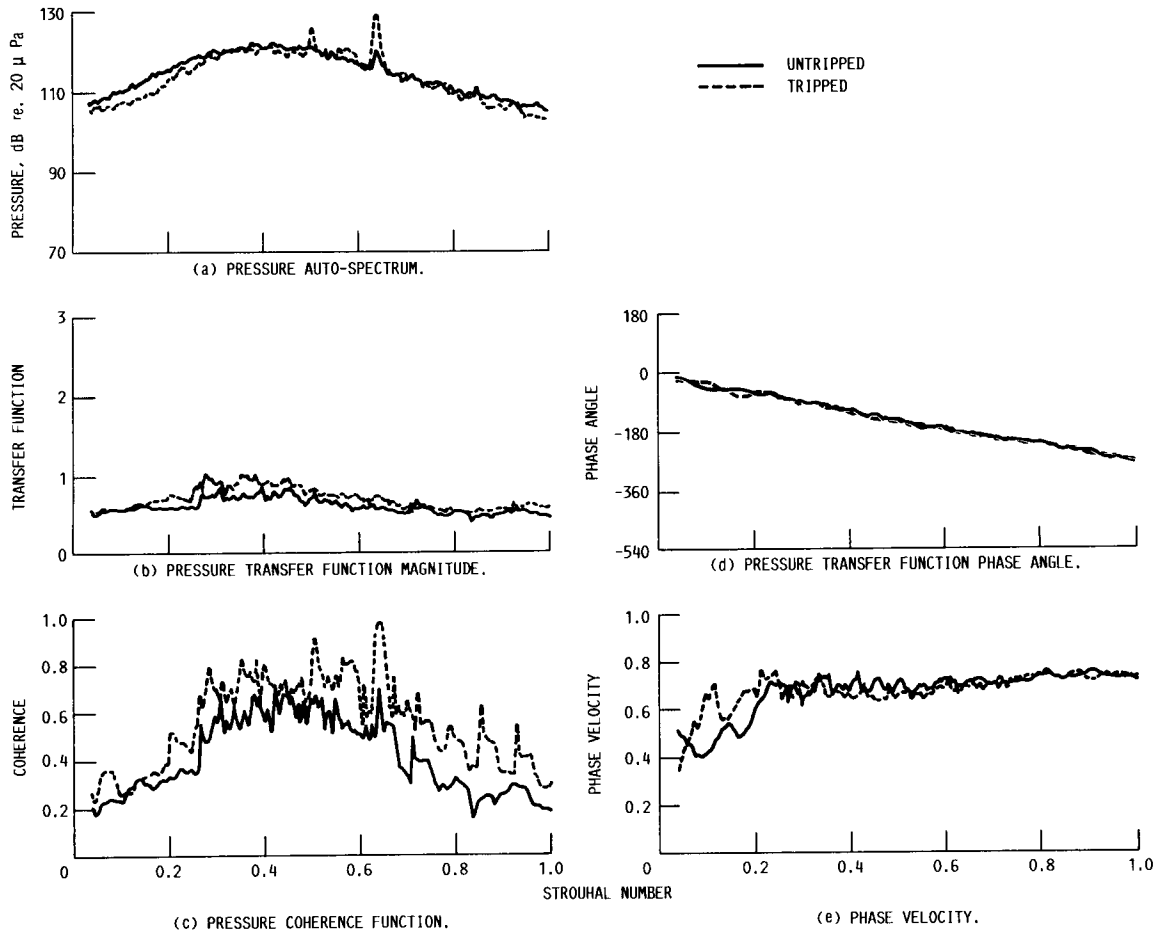

(a) PRESSURE AUTO-SPECTRUM.

(b) PRESSURE TRANSFER FUNCTION MAGNITUDE.

(d) PRESSURE TRANSFER FUNCTION PHASE ANGLE.

(c) PRESSURE COHERENCE FUNCTION.

(e) PHASE VELOCITY.

FIGURE 5. - MEASUREMENTS AT x/d = 3. (r/d = 0, M = 0.3.)

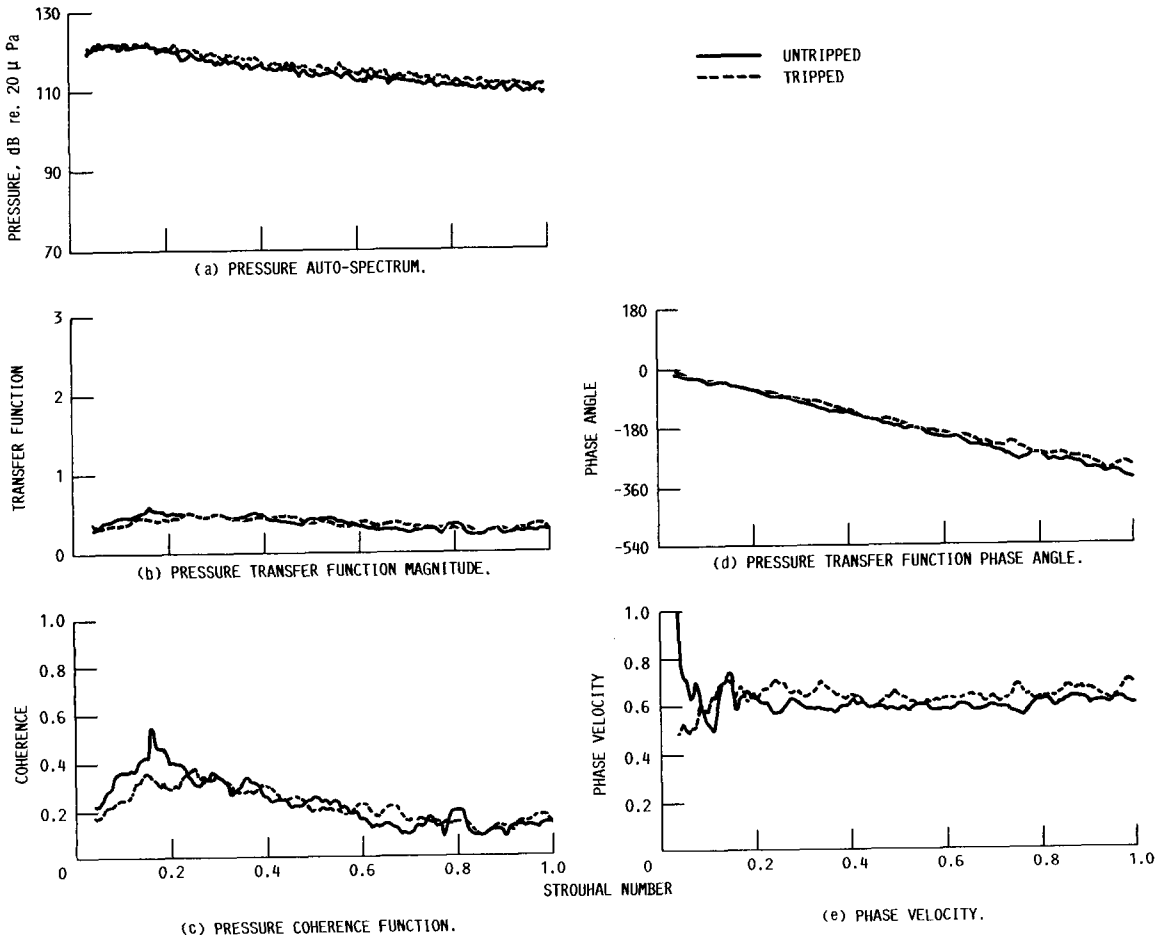

FIGURE 6. - MEASUREMENTS AT x/d = 9. (r/d = 0, M = 0.3.)

NASA
National Aeronautics and Space Administration

Report Documentation Page

1. Report No.	2. Government Accession No.	3. Recipient's Catalog No.
NASA TM-100915		

4. Title and Subtitle
Initial Condition Effect on Pressure Waves in an Axisymmetric Jet

5. Report Date
May 1988

6. Performing Organization Code

7. Author(s)
Jeffrey H. Miles and Ganesh Raman

8. Performing Organization Report No.
E-4076

10. Work Unit No.
505-62-21

9. Performing Organization Name and Address
National Aeronautics and Space Administration
Lewis Research Center
Cleveland, Ohio 44135-3191

11. Contract or Grant No.

13. Type of Report and Period Covered
Technical Memorandum

12. Sponsoring Agency Name and Address
National Aeronautics and Space Administration
Washington, D.C. 20546-0001

14. Sponsoring Agency Code

15. Supplementary Notes
Prepared for the First National Fluid Dynamics Congress cosponsored by the AIAA, ASME, ASCE, SIAM, and APS, Cincinnati, Ohio, July 24-28, 1988. Jeffrey H. Miles, NASA Lewis Research Center; Ganesh Raman, Sverdrup Technology, Inc., (Lewis Research Center Group), NASA Lewis Research Center, Cleveland, Ohio 44135.

16. Abstract
A pair of microphones (separated axially by 5.08 cm and laterally by 1.3 cm) are placed on either side of the jet centerline to investigate coherent pressure fluctuations in an axisymmetric jet at Strouhal numbers less than unity. Auto-spectra, transfer-function, and coherence measurements are made for a tripped and untripped boundary layer initial condition. It was found that coherent acoustic pressure waves originating in the upstream plenum chamber propagate a greater distance downstream for the tripped initial condition than for the untripped initial condition. In addition, for the tripped initial condition the development of the coherent hydrodynamic pressure waves shifts downstream.

17. Key Words (Suggested by Author(s))	18. Distribution Statement
Hydrodynamic pressure waves; Coherent pressure measurements; Jet shear layer; Tripped boundary layer; Untripped boundary layer	Unclassified – Unlimited Subject Category 34

19. Security Classif. (of this report)	20. Security Classif. (of this page)	21. No of pages	22. Price*
Unclassified	Unclassified	12	A02

*For sale by the National Technical Information Service, Springfield, Virginia 22161